

# In-plane seismic behaviour of ashlar three-leaf stone masonry walls: Verifying performance limits

Meta Kržan & Vlatko Bosiljkov

To cite this article: Meta Kržan & Vlatko Bosiljkov (2021): In-plane seismic behaviour of ashlar three-leaf stone masonry walls: Verifying performance limits, International Journal of Architectural Heritage, DOI: [10.1080/15583058.2021.1963504](https://doi.org/10.1080/15583058.2021.1963504)

To link to this article: <https://doi.org/10.1080/15583058.2021.1963504>



© 2021 The Author(s). Published with license by Taylor & Francis Group, LLC.



Published online: 09 Sep 2021.



Submit your article to this journal [↗](#)



Article views: 615



View related articles [↗](#)



View Crossmark data [↗](#)



Citing articles: 2 View citing articles [↗](#)

# In-plane seismic behaviour of ashlar three-leaf stone masonry walls: Verifying performance limits

Meta Kržan<sup>a</sup> and Vlatko Bosiljkov<sup>b</sup>

<sup>a</sup>The Department of Structures, Slovenian National Building and Civil Engineering Institute, Ljubljana, Slovenia; <sup>b</sup>Faculty of Civil and Geodetic Engineering, University of Ljubljana, Ljubljana, Slovenia

## ABSTRACT

In light of the forthcoming second generation Eurocodes (EC), the results of conducted systematic in-plane cyclic and compressive tests on three-leaf stone masonry walls are discussed following new requirements and provisions. The new proposal for EC8-3 for existing buildings is based on partial factors safety approach, though it considers different uncertainties in defining input parameters for effective seismic performance-based assessment. Prior to its application, massive calibration effort will be needed since there is no standardized method for shear testing of masonry walls. In this paper, the performance limit states damage, resistance, and displacement capacities from conducted test results were evaluated and assessed through comparison with analytical solutions and imposed limit values, as stated in existing codes. The test results provide a much higher deformation capacity than the limits provided in both existing and new proposal of EC8-3 as well as those in the ASCE code provisions. The reason for this lies in the soft, “ductile” mortar for which the presumed resistance according to code provisions should be significantly higher when considering good quality ashlar three-leaf stone masonry.

## ARTICLE HISTORY

Received 1 March 2021  
Accepted 29 July 2021

## KEYWORDS

Analytical formulations; code provisions; model error; multi-leaf stone masonry; performance limits; proposals for new Eurocodes; seismic performance

## 1. Introduction

For the analysis and design of stone masonry structures, current Eurocode provisions for existing buildings do not differentiate between single- and multi-leaf walls and the analytical models for determination of mechanical parameters being provided are valid only for solid masonry (EN 2005-3: 2005 2005). Thus, for the assessment of the shear behavior of in-plane laterally loaded multi-leaf walls for the purpose of effective seismic PBA (Performance-based Assessment) of architectural heritage structures, the same analytical models as those for single-leaf walls are used. Existing EC8-3 consider two failure mechanisms—shear mechanism based on the Mohr–Coulomb model and flexural mechanism. The former one is not suitable for irregular masonry, thus the most common models for this type of masonry for determining the shear resistance are models for diagonal failure by Turnšek and Čačovič (1971) based on phenomenological approach and for shear failure by Mann and Müller (1982) based on several criteria's including the Mohr–Coulomb model for the sliding mechanism. These models have already been incorporated in some national codes (DIN 1053-1: 1996-11 1996; NTC 2018 2009) together with the model for

flexural resistance that is also adopted in the new emerging version of Eurocode 8–3 (EN1998-3 SC8 06-10-2019 2019).

For nonlinear analysis, the drift (rotation) capacity of walls is, for various damage limit states in current code provisions EC8-3 (EN 2005-3: 2005 2005) and ASCE/SEI 41–06 (based on former FEMA 356 (ASCE/SEI 41–06 2007)) among others, provided in dependence of two failure mechanisms (i.e., shear or flexural). Imposed limits differ in dependence from geometry and boundary conditions of the elements. The new EC8-3 proposal considers three failure mechanisms (flexural, shear sliding, and diagonal cracking mechanism) for regular masonry, while the shear sliding mechanism is omitted in the case of irregular masonry.

Unlike existing EC8-3, the new proposal considers different shapes of nonlinear capacity curves. Apart from the bi-linear curve, there are numerous multi-linear options with different possibilities for modeling post-peak behavior of both piers' and spandrels' masonry structural elements.

Regarding the effective stiffness to be presumed for the initial part of the multi-linear response curves to be adopted in models, it was confirmed by Vanin et al. (2017) that the estimation of stiffness characteristics has great uncertainty, as the experiments considered in

the study show 2–3 times higher variation for effective stiffness compared to the predicted strength characteristics. The authors analyzed the results of 16 different experimental campaigns of stone masonry walls, varying in wall typology and testing (both diagonal compression as well as shear tests, monotonic and cyclic, laboratory, and in-situ were considered).

The new EC8-3 proposal (EN1998-3 SC8 06-10-2019 2019) is in agreement with the general framework of Eurocodes and is based on the partial factors safety format. It considers different (both aleatoric and epistemic) uncertainties in defining input parameters for effective PBA provided in the form of a bias factor and dispersion parameters. Its output, however, is not in a probabilistic format. It requires single final analysis, prior to which a so-called “sensitivity” analysis of the structure’s response is foreseen in order to identify the most influencing parameters (materials, details, and geometry) and properly set a degree of belief for each of them. Depending on the results of preliminary sensitivity analysis, further in-situ investigation could be optimized in order to properly set the knowledge levels for input parameters. Prior to its implementation, this new approach requires a massive calibration effort, that is yet to be done, before the new proposal of EC8-3 becomes operational (Franchin, Pinto, and Rajeev 2010).

Apart from considering different knowledge levels for material, details, and geometry through partial factors, all mechanical and deformation parameters for the PBA, according to new proposal of EC8-3, are provided as mean values together with their coefficients of variation. This approach is eligible if there

are standardized methods for evaluation of both mechanical parameters and performance limit states for masonry structural elements. However, it may be a debating issue if there are no standardized methods to evaluate behaviour and performance limits for laterally in-plane loaded masonry walls. From this perspective, the results of the experimental tests (presented in detail in (Kržan and Bosiljkov 2021)) were compared and discussed, considering the provisions stated in the main part as well as in the Annex E of the new proposal of EC8-3.

### 1.1. Summary of conducted own experimental tests

An extensive experimental laboratory campaign including 2 compression and 15 cyclic shear tests on full size three-leaf stone masonry piers (100/40/150 cm<sup>3</sup>) was conducted together with tests on the constituents. Test setup for cyclic shear tests with specimen is presented in Figure 1. The external leaves of 15 cm average thickness were constructed of regularly coursed, squared, and roughly tooled ashlar limestone and low strength lime mortar with joints of 2.0 cm average thickness, while the internal core of 10 cm approximate thickness was filled with stone rubble and lime mortar with low percentage of voids. Lime mortar compressive strength at start of testing was 1.88 MPa while average compressive strength of stone-cube specimen cut from stone units was 171.5 MPa. Half of the specimens had header stones going through the whole depth of the specimen, which, however, proved not to significantly influence the



Figure 1. Test setup for cyclic shear test.

**Table 1.** Specimen characteristics, shear tests combinations, and the failure mechanisms of walls and displacements ( $d_i$ ) and resistances ( $F_i$ ) obtained in various characteristic limit states in cyclic shear tests of walls with mean values and coefficient of variation (CV).

Test	Vert. load [% $f_{Mc}$ ]	Boundary conditions	No. of rows of stone	Failure mechanism	First shear crack				Maximum force				Maximum displacement			
					$d_{cr}$ [mm]	mean (CV)	$F_{cr}$ [kN]	mean (CV)	$d_{Fmax}$ [mm]	mean (CV)	$F_{max}$ [kN]	mean (CV)	$d_{max}$ [mm]	mean (CV)	$F_{dmax}$ [mm]	mean (CV)
1-SPk-5-1	5	cantilever	11	Rocking	0.00		0.0		49.6		42.1		49.8		41.2	
1.2-SPk-7.5-1	7.5	cantilever	11	Rocking	34.70	26.0(-)	57.7	54.8(-)	69.5	63.8(-)	68.5	65.2(-)	69.7	64.8(-)	66.1	63.2(-)
2-SNk-7.5-1	7.5	cantilever	11	Rocking	17.37		51.9		58.1		61.8		59.8		60.3	
3-SNv-7.5-1	7.5	fixed-fixed	11	Mixed	7.44	8.27* (14)	61.2	65.0* (9)	22.3	25.6* (12)	88.2	105.7* (12)	24.9	28.2* (8)	73.0	77.2* (24)
4-SPv-7.5-1	7.5	fixed-fixed	11	Mixed	7.45		60.9		29.7		119.9		29.9		101.7	
5-SNv-7.5-2	7.5	fixed-fixed	11	Mixed	9.93		73.0		24.7		109.0		29.9		83.3	
6-SPv-7.5-2	7.5	fixed-fixed	10	Mixed	7.45		60.2		9.9		61.9		14.9		50.8	
7-SPv-15-1	15	fixed-fixed	11	Shear	2.98	3.23 (34)	81.4	70.1 (20)	14.8	14.8 (6)	129.2	123.0 (3)	19.9	21.1 (6)	81.9	91.7 (7)
8-SNv-15-1	15	fixed-fixed	12	Shear	4.96		85.7		14.9		121.2		22.4		90.3	
9-SPv-15-2	15	fixed-fixed	11	Shear	1.98		52.5		16.1		122.1		22.4		93.6	
10-SNv-15-2	15	fixed-fixed	12	Shear	2.98		60.9		13.4		119.4		19.9		100.8	
11-SNk-15-1	15	cantilever	11	Shear	2.98	3.48 (25)	68.3	72.7 (10)	15.0	18.1 (25)	114.5	118.7 (4)	22.4	24.9 (24)	98.6	103.0 (4)
12-SPk-15-1	15	cantilever	11	Shear	2.98		65.8		15.2		114.0		22.4		100.9	
13-SPk-15-2	15	cantilever	11	Shear	2.98		72.2		16.2		122.5		19.9		104.7	
14-SNk-15-2	15	cantilever	11	Shear	4.97		84.5		26.0		123.7		34.9		108.0	

\*Test no. 6 is not considered in the calculation of average results. Letters N or P in the test name relate to morphology (N — without and P — with header stones).

**Table 2.** Literature reference  $f_{Mc}$  values and values calculated according to various analytical models.

$f_{Mc}$ [MPa]		Analytical models					
Literature values		Analytical models					
NTC 2018* (2018) (Italy)	PIET 70 (1971) (Spain and Portugal)	Slovenia (Bosiljkov et al. 2004)	Croatia (Aničić et al. 1989)	Egermann (1993)	Binda et al. (2006)	Tassios and Chronopoulos (1986); Tassios (2004)	Tassios and Chronopoulos (1986); Tassios (2004) (single-leaf) 1986
dressed	rectangular stone	ashlar masonry with $h_b < 30$ cm and $f_{bc} > 100$ MPa	ashlar roughly tooled multi-leaf	uncoursed three-leaf wall filled with rubble			
6.0 (min)	4.0	1.2 (min)	4.7 (min)	3.44 (*)	4.73 (*)	2.66 (+)	6.51 (+)
8.0 (max)		1.6 (max)	5.5 (max)	4.49 (**)	6.23 (**)	1.42 (++)	6.75 (++)

$h_b$  denotes masonry unit (block) height,  $f_{bc}$  compressive strength of the unit, (\*) and (\*\*) denote results considering compressive strength of external leaves as min and max values for dressed rectangular masonry according to NTC 2018 (NTC 2018 2018), respectively.

response for the tested type of walls under compression or shear loading in terms of strength and deformation capacity obtained.

Compression tests on two walls with different morphology provided average compressive strength, elastic, and shear modulus equal 6.05 MPa, 968 MPa, and 383 MPa, respectively.

**Table 3.** Proposed mechanical characteristics for squared stone masonry.

	$f_{Mc}$ [MPa]	$f_{Mt}$ [MPa]	$f_{v0}$ [MPa]	$E_M$ [MPa]	$G_M$ [MPa]
Mean value	7.00	~*	0.220	2800	860
CV	0.14	-	0.14	0.14	0.09

in NTC 2018  $f_{Mt} = 1.5 f_{v0}$

Results of cyclic shear tests, relevant for the presented paper, are summarized in Table 1. To obtain different failure mechanism and to study and verify shear behavior performance limits under various conditions: two variations of boundary conditions were imposed (cantilever and fixed-fixed) and three different levels of constant vertical loads were applied on the walls during shear testing, i.e. 5.0, 7.5, and 15.0% of compressive strength of masonry  $f_{Mc}$ . In Table 2, the damage mechanisms obtained in tests are presented and lateral resistance and displacements obtained for characteristic limit states (first shear crack ( $F_{cr}$ ,  $d_{cr}$ ), maximum resistance ( $F_{max}$ ,  $d_{Fmax}$ ), and maximum displacement ( $F_{dmax}$ ,  $d_{max}$ ))

are provided for each test together with average results for the specific combination of vertical load and boundary conditions.

## 2. Mechanical properties for multi-leaf masonry

### 2.1. Compressive strength and stiffness properties

Although multi-leaf masonry is properly addressed in contemporary masonry codes, this topic has never reached some consensus among researchers regarding historical masonry. To evaluate compressive strength  $f_{Mc}$  of multi-leaf masonry, Egermann (1993) proposed a simplified model (Equation 1) based on the Binda et al. (1992) “spring” model and the results of experimental tests:

$$f_{Mc} = 2 \frac{t_1}{2t_1 + t_2} \theta^e f_{Mc}^e + \frac{t_2}{2t_1 + t_2} \theta^i f_{Mc}^i \quad (1)$$

The value  $t_1$  represents the thickness of the external leaf, while  $t_2$  represents the thickness of the internal (infill) leaf;  $\theta^e$  and  $\theta^i$  present correction coefficients for the external  $f_{Mc}^e$  and internal  $f_{Mc}^i$  leaf's compressive strength, respectively. The coefficient  $\theta^e$  depends on the bending stiffness of the external leaf, the boundary conditions and the bending moments, and is smaller than 1.0 due to  $f_{Mc}^e$  never being reached as a consequence of horizontal loading through the yielding infill. The coefficient  $\theta^i$  represents the ratio between the component stress at failure, and the uniaxial compressive strength of the infill. Since the lateral deformations of the infill are hindered by the outer leaves, and the vertical loading induces a tri-axial compressive stress state,  $\theta^i$  is larger than one and depends on the stratification of the infill.

Binda et al. (2006) provided a solution considering different hypotheses of the external load supports:

the external load is completely supported by the stiffer elements, i.e., the outer-leaves (Equation 2),

the external load is supported by each leaf according to its cross-section area ratio (Equation 3), and

the external load is supported by each leaf according to its area ratio and adjusted by a correction factor (Equation 1):

$$f_{Mc} = 2 \frac{t_1}{2t_1 + t_2} f_{Mc}^e, \quad (2)$$

$$f_{Mc} = 2 \frac{t_1}{2t_1 + t_2} f_{Mc}^e + \frac{t_2}{2t_1 + t_2} f_{Mc}^i \quad (3)$$

For three-leaf masonry with keyed collar joints and ashlar masonry in the outer leaves, the authors proposed correction factors  $\theta^e$  and  $\theta^i$  equal to 0.7 and 1.3, respectively.

Greek authors Tassios and Chronopoulos (Tassios 2004; Tassios and Chronopoulos 1986) determined the  $f_{Mc}$  of a multi-leaf historic masonry (Equation 4) based on the compressive strength of units and mortar  $f_{bc}$  and  $f_{mc}$ , thickness of the joints, shape of the units, and type of masonry (stone or brick) (Equation 5):

$$f_{Mc} = 2 \frac{t_1}{2t_1 + t_2} f_{Mc}^e + \frac{t_2}{2t_1 + t_2} f_{Mc}^i \quad (4)$$

$$f_{Mc}^e = \left( \frac{2}{3} \sqrt{f_{bc}} + k_1 f_{mc} - k_2 \right) / \xi_e \quad (5)$$

$$\xi_e = 1 / (1 + 3.5(k - k_0)) \quad (6)$$

$$f_{Mc}^i = f_0 e^{(-10n_i)} \xi_i \quad (7)$$

$$\delta = t_1 / t_2 \quad (8)$$

$$\lambda_e = 1 - \left[ \frac{0.018}{f_{Mc}^e} \left( \frac{h_w}{t_2} \right)^2 h_w^{2/3} \right] \cdot \left[ \frac{0.31(h_w/t_2)^3}{E_1} + \frac{t_2}{E_2} \right] \approx 1 - 0.06 \zeta_e t_1 h_w^{-4/3} \quad (9)$$

$$E_1 = \zeta_1 f_{Mc}^e \quad (10)$$

$$E_2 = \zeta_2 f_{Mc}^i \quad (11)$$

In Equations 4–11,  $k_0$ ,  $k_1$ , and  $k_2$  are coefficients dependent on the type and shape of the units: 0.3, 0.6, and 2.5 for rubble stones, 0.2, 0.3, and 0.5 for cut stones, 1.0, 0.2, and 0.0 for ashlar stone blocks, and 0.3, 1.0, and 0.0 for bricks, respectively.  $k$  represents the proportion of mortar in the masonry by volume and  $\xi_e$  describes the bed-joint thickness and the volume of the included mortar. For evaluation of elastic moduli of external and internal leaves,  $\zeta_1$  is equal to 500 for rubble, 1000 for cut, and 1500 for ashlar masonry, whereas  $\zeta_2$  is equal to 2000;  $\lambda_i$  is equal to 1,  $f_0$  depends on the mortar compressive strength  $f_{mc}$  and is 35 MPa for  $f_{mc} \sim 10$  MPa, 20 MPa for  $f_{mc} \sim 4$  MPa, and 10 MPa for  $f_{mc} \sim 1$  MPa. The value  $n_i$  is the porosity of core stones,  $\xi_i$  is equal to 1.0 if the filling is made of larger or medium-sized blocks where gaps are filled with mortar, otherwise its value is 0.0. In Equation 9,  $t_1$ ,  $h_w$  are inserted in [mm].

Furthermore, Egermann (1993) proposed the elasticity modulus of multi-leaf walls to be calculated according to Equation 12. Eurocode provision EC6 (EN 1996-1-1: 2005 2005) prescribes that in the absence of experimental tests, the  $E_M$  is determined as 1000  $f_{Mc}$ . In the literature, this ratio ( $E_M/f_{Mc}$ ) may range between 500

and 1000, with a lower bound range of 80–140  $f_{Mc}$  (Bosiljkov, Totoev, and Nichols 2005; Elmenshawi et al. 2011; Tomažević 1999):

$$E_M = \frac{2t_1}{t_w} E_1 + \frac{t_2}{t_w} E_2 \quad (12)$$

The new proposal of the EC8-3 (Annex E) provides a procedure for the assessment of the compressive strength of multi-leaf walls, where the inner core represents a substantial part of the cross-section. The methodology reflects outcomes from double flat-jack tests. For three-leaf walls with unequal thicknesses of outer leaves ( $t_1$  and  $t_3$  are the thickness of the two external leaves, while  $t_2$  is the thickness of the inner core), the compressive strength is provided as (Equation 13):

$$f_{Mc} = \begin{cases} E_M \varepsilon_r & \text{if } \varepsilon_r \leq f_{Mc}^i / E_2 \\ [(t_1 E_1 + t_3 E_3) \varepsilon_r + t_2 f_{Mc}^i] / t & \text{if } \varepsilon_r > f_{Mc}^i / E_2 \end{cases} \quad (13)$$

The strain  $\varepsilon_r$  should be calculated at the attainment of the weakest external leaf's maximum strength ( $\varepsilon_r = \min(f_{Mc}^1/E_1; f_{Mc}^3/E_3)$ ). However, as stated in the new proposal, in the case of negligible material properties of the inner core the equivalent properties of the masonry panel should be directly obtained from those of the external leaves by multiplying them with the ratio between effective thickness (external leaves) and total thickness (factor  $(t_w - t_2)/t_w$ ). In Italian code NTC 2018 (2018) this reduction is necessary in case of core thickness larger than 30% of the overall thickness of the wall. The moduli  $E_M$  and  $G_M$  should be calculated as  $X$  in Equation 14:

$$X = \frac{t_1 X_1 + t_2 X_2 + t_3 X_3}{t_w} \quad (14)$$

where  $X_i$  are the moduli of three different leaves.

In most masonry codes (including EC6), the shear modulus  $G_M$  is prescribed as a fraction of  $E_M$ . A simple design assumption of Poisson's ratio ( $\nu_M = 0.25$ ) and of

the isotropic material leads to the estimation:  $G_M = 0.4 E_M$ . By considering the orthotropic nature of masonry, through the application of homogenization procedures, the adoption of lower ratios could also be justified, such as  $G_M = E_M/3$ ; this latter ratio is assumed for the reference values proposed in NTC 2018 (2018) and also supported by the results of some experimental campaigns (e.g., those illustrated in Magenes et al. (2010) related to the response of undressed double-leaf stone masonry walls).

The shear modulus determined according to these ratios relates to the uncracked or intact masonry. For seismic design purposes,  $G_M$  should be reduced to a value of 5–25% of  $E_M$  (Bosiljkov, Totoev, and Nichols 2005; Elmenshawi et al. 2011; Tomažević 1999). In the proposal of EC8-3, reference values of  $G_M$  are provided in Annex E in dependence of the type of masonry, if in-situ tests on the building are not conducted (for this purpose diagonal compression test is encouraged).

## 2.2. Evaluation of compression test results through comparison with literature values and analytical models

To validate the  $f_{Mc}$  of the walls obtained in the tests, Table 4 presents the limit values provided in the literature and code provisions for masonry typology which are similar to the ones of the tested walls and values obtained through analytical models (Binda et al. 2006; Egermann 1993; Tassios 2004; Tassios and Chronopoulos 1986). For calculation according to the Egermann and Binda et al. models, the min<sup>(\*)</sup> and max<sup>(\*\*)</sup> values considered for the compressive strength of external leaves were in accordance with NTC 2018 (2018). Among all of the recommendations, this code provides the most structured values with regard to the type of masonry. For the inner infill layer, the results considered came from core compression tests conducted

**Table 4.** Analytically calculated shear resistances  $V_R$  for tested piers considering various failure mechanisms models for gross and net cross section area  $V_{R,net}$  (in brackets) together with experimentally obtained averaged idealized shear resistance  $F_{id}$ .

Pre-compression level, boundary conditions	$V_{R,r}$ [kN]	$V_{R,d}$ [kN]		$V_{R,dj}$ [kN]		$V_{R,du}$ [kN]	$V_{R,s}$ [kN]	$F_{id}$ [kN]	Failure mechanism
		NTC min	NTC max	( $b = 1.5$ )	( $b = 1.0$ )				
7.5% $f_{Mc}$ cantilever	54.9 (53.2)	74.9 (63.0)	89.8 (74.9)	34.2 (45.0)	45.0 (43.9)	6659	90.0(67.5)	57.8	rocking
7.5% $f_{Mc}$ fixed-fixed	109.7 (106.3)	74.9 (63.0)	89.8 (74.9)	37.1 (34.3)	46.4 (51.1)	6549	105.0 (101.3)	100.2*	mixed
15% $f_{Mc}$ cantilever	102.2 (95.3)	101.5 (86.5)	119.6 (101.5)	63.4 (61.2)	93.4 (87.8)	6538	187.5 (187.5)	113.7	shear
15% $f_{Mc}$ fixed-fixed	205.4 (190.6)	101.5 (86.5)	119.6 (101.5)	65.0 (62.1)	97.5 (93.7)	6495	202.5 (198.8)	112.6	shear

\* the mean  $F_{id}$  for 7.5%  $f_{Mc}$  vertical load and cantilever boundary conditions calculated for 3 tests with an average horizontal bed joint thickness of 15 mm. Test no. 6 is not included;  $F_{id}$  equal to 57.4 kN was obtained for test no. 6.

within the experimental campaign on cylinder samples (compressive strength of 0.90 MPa). For the Tassios et al. models (Tassios 2004; Tassios and Chronopoulos 1986), the recommended coefficients for cut stone masonry<sup>(+)</sup> as well as for ashlar masonry<sup>(++)</sup> were considered in the analysis.

The obtained results coincide well with the NTC 2018 minimum values for dressed rectangular stone. The texture of the walls in NTC 2018 also corresponds to the tested walls. The reason for being on lower bound could be due to a significant thickness of mortar joints (with regard to dressed masonry).

Results calculated according to analytical models vary considerably. Analytical models for three-leaf masonry all underestimate the  $f_{Mc}$  of the tested walls. This is probably due to a very good connection between the internal and external leaves, which prevents the out-of-plane failure. Formulation of Tassios and Chronopoulos (Tassios 2004; Tassios and Chronopoulos 1986) for estimation of  $f_{Mc}$  of single-leaf masonry provides the closest estimation but it is not on the safe side; it overestimates  $f_{Mc}$  by 7.6%. The results confirm that the analytical model provided in EC6 is not appropriate for historic masonry with low mortar strength, since  $f_{Mc}$  is significantly overestimated (19.9 MPa). Provisions from the new proposal of EC8-3 for negligible material properties of the inner core would reduce the presumed compressive strength of the external leaves by a factor of 0.75 (ratio  $(t_w - t_2)/t_w$ ).

Contrary to compressive strength, the obtained stiffness characteristics are significantly lower compared to NTC 2018 values, where  $E_M$  ranges between 2400 and 3200 MPa and  $G_M$  between 780 and 940 MPa. The values in the new proposal of EC8-3 are based on NTC 2018 min and max values and derived as mean values.

### 2.3. Shear resistance

In the new proposal of EC8-3 provisions, the shear resistance of masonry walls is defined as dependent on whether the structural element is pier or spandrel. Shear sliding, diagonal cracking, and flexural analytical formulations are provided for piers with regular masonry (modern and pre-modern masonry with regular texture and morphology). For masonry with an irregular pattern (pre-modern masonry), however, only the flexural and diagonal cracking failures are foreseen. Resistance is determined as the lower bound from proposed analytical formulations for different mechanisms.

Since our masonry walls were designed to represent old historical (pre-modern), good-quality masonry—consequently, the texture and morphology of the masonry were regular, with proper overlapping of

units. Thus, in our analytical study, the design shear resistance  $V_R$  was evaluated according to the requirements for regular masonry considering different criteria for the diagonal failure mechanism.  $V_R$  was calculated by considering the mean values for mechanical properties of masonry according to the NTC 2018, without any reduction due to material or any other uncertainties. Shear resistance  $V_{R,r}$  denotes the shear resistance resulting from flexural mechanism (Equation 15),  $V_{R,d}$  from diagonal cracking mechanism (Equation 16),  $V_{R,dj}$  from diagonal cracking mechanism with diagonal cracking through joints (Equation 17), and  $V_{R,s}$  from sliding mechanism (Equation 18):

$$\theta_{NC} = \frac{4}{3} \eta (1 - \sigma_0 / f_{Mc}) \quad (15)$$

$$V_{R,d} = l_w t_w \frac{f_{Mt}}{b} \sqrt{\left(1 + \frac{\sigma_0}{f_{Mt}}\right)} \quad (16)$$

$$V_{R,dj} = \frac{l_{wc} t_w}{b} \left( \frac{f_{v0}}{1 + \mu_{fr} \varphi} + \frac{\mu}{1 + \mu_{fr} \varphi} \sigma_d \right) \quad (17)$$

$$V_{R,s} = l_{wc} t_w (f_{v0} + \mu_{fr} \sigma_d) \quad (18)$$

In equations above,  $t_w$ ,  $l_w$ , and  $h_w$  present the thickness, length, and height of the wall, respectively,  $\sigma_0$  is the level of pre-compression in the middle cross section in Equation 15, the parameter  $\psi$  is the correction coefficient dependent on boundary conditions equal to 1 for cantilever and to 2 for both fixed ends walls;  $f_{Mt}$  is the diagonal tensile strength of the masonry,  $b$  is the shear distribution factor,  $f_{v0}$  is the masonry initial shear strength, and  $\mu_{fr}$  is the coefficient of friction (in new EC8-3 proposed as 0.5);  $\varphi$  is the interlocking parameter considering the texture of the masonry,  $l_{wc}$  the length of the compressed part of the wall, and  $\sigma_d$  the average vertical stress in the compressed part of the wall.

For the verification of a structural element's capacity regarding design demand obtained from the chosen type of analysis, the design shear resistance  $V_{Rd}$  should be calculated in accordance with the knowledge level. For non-linear analysis it is proposed as

$$V_{Rd} = V_R / \gamma_{Rd}, \quad (19)$$

where  $V_R$  is the shear force obtained from the analytical models and  $\gamma_{Rd}$  is a factor accounting for uncertainties regarding model error, and is defined for the ultimate resistance (drifts) in dependence of different knowledge levels of details (KLD), geometry (KLG), and materials (KLM). The reduction factor should encompass uncertainties in evaluating resistance by using the mean values of all input variables and considering a lower fractile of the

resistance distribution. This approach should eliminate statistical uncertainty of estimation as a consequence of limited sample size and the model error of analytical formulations. The reduction factor in connection to the knowledge on the material is in the range of 1.65–2.15 for flexural mechanisms, 1.35–1.65 for sliding mechanisms, and 1.35–1.55 (irregular masonry) and 1.40–1.70 (regular masonry) for diagonal mechanisms. Within proposed limits, particular values for reduction factors are defined according to the three levels of knowledge, (C-comprehensive, E-extended, and L-limited), where the above-mentioned lower- and upper-range limits refer to C and L knowledge levels.

In the annex of the new EC8-3 proposal, the reference values for mechanical properties of different masonry types are also provided through mean values and coefficient of variation (CV). The mean values are derived from NTC 2008 (2009), by considering the min and max values for mechanical properties. Table 3 provides the values from the annex (with CV) for our type of masonry.

#### 2.4. Evaluation of shear test results in comparison with analytical models

The results of the analysis are presented in Table 4, where the averaged idealized shear resistances of walls  $F_{id}$  from tests with the same boundary conditions and vertical load are summarized. The criterion for evaluating the resistance in the case of diagonal cracking through joints  $V_{R,dj}$  (Mann and Müller 1982) produced the lowest results in all cases. The average masonry unit length, equal to 20 cm, was considered while calculating the results. While the cracking through joints occurred in almost all of the experimental tests, the estimated  $V_{R,dj}$  values were significantly smaller compared to the resistances obtained in all tests—apart from test no. 6. Subsequently, one of the conclusions is that the diagonal

joint criterion underestimates the resistance in case of weak, ductile mortars with normal joint thicknesses (joint thickness of the tested masonry was 10–25 mm). The results for  $V_{R,dj}$  are less conservative if a value of 1.0 (instead of 1.5) is considered for  $b$ .

For the calculation of  $V_{R,d}$  (i.e., diagonal cracking resistance (Turnšek and Čačovič 1971)), the lower and upper limit of  $f_{Mt}$  provided in NTC 2018 code provisions (0.135 and 0.18 MPa) were considered. The diagonal cracking model produced the most accurate results for tests in which the diagonal shear mechanism occurred. The results were non-conservative for the higher pre-compression level if the upper limit  $f_{Mt}$  was considered (though for less than 10% except for test no.6). It has to be noted that, for cantilever boundary conditions and a higher pre-compression level, the results indicate a rocking failure prior to the diagonal cracking failure of the wall ( $V_{R,r}$  and  $V_{R,d}$  are 93.9% and 106.4% of  $F_{id}$  considering the upper limit of  $f_{Mt}$ , respectively). The diagonal cracking through the units  $V_{R,du}$  (Mann and Müller 1982) provided very conservative results due to a very high compressive strength of the stone. Shear resistance  $V_{R,ss}$ , which considers the sliding mechanism according to the Mohr–Coulomb criterion, was also evaluated but was never critical.

In case of the occurrence of diagonal cracking and rocking, it can be concluded that  $V_{R,d}$  and  $V_{R,r}$  adequately estimate the design resistance—provided that the  $f_{Mt}$  is properly estimated and the mortar joints are of normal thicknesses. This does not hold for test no. 6 where all of the criteria, except for diagonal cracking through the joint ( $V_{R,dj}$ ), highly overestimate the obtained resistance.

Ratios of  $V_R$  calculated according to various criteria and normalized versus  $F_{id}$  (obtained from tests) are presented in Figure 2.

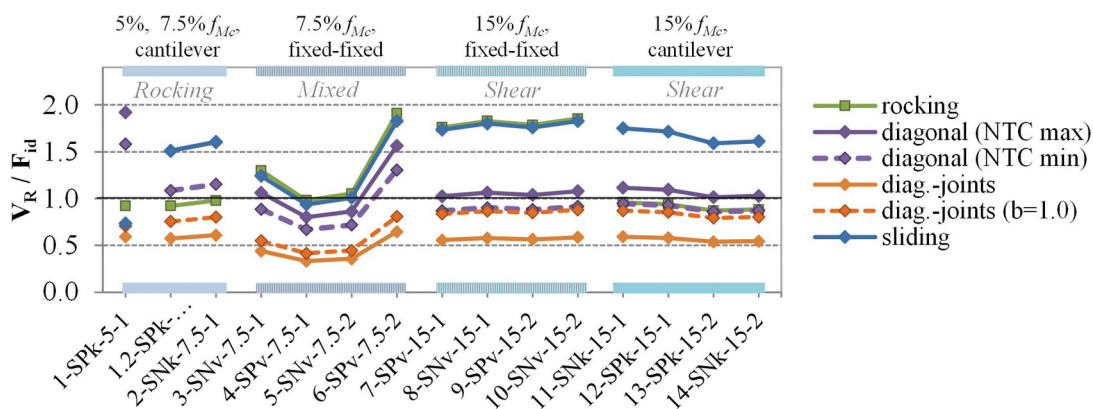


**Figure 2.** Ratio between analytically calculated shear resistances  $V_R$  for various failure mechanisms and idealized shear resistances  $F_{id}$  obtained from tests.

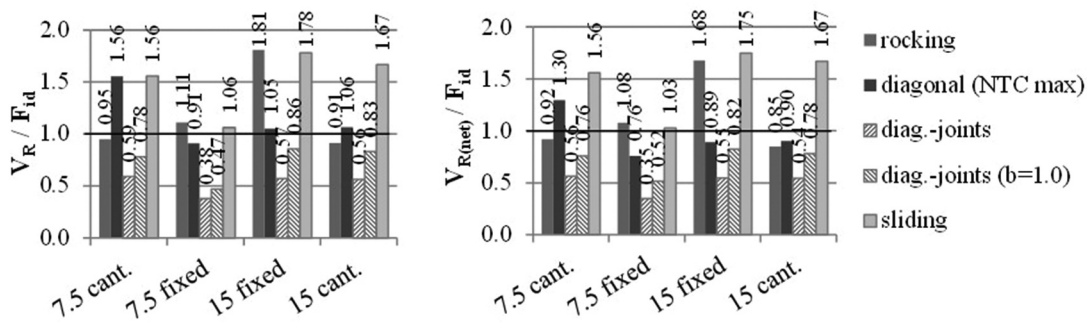


**Figure 3.** The average ratio between analytically calculated shear resistances  $V_R$  and idealised experimental shear resistance  $F_{id}$  for tests with the same boundary conditions and vertical load, obtained for the entire cross section (left) and the reduced cross section (right).

From the comparisons of  $V_R$  calculated considering the entire wall cross section versus net cross section  $V_{R,net}$  (only external leaves, results presented in Table 4), it may be concluded that for three-leaf masonry, where the inner core is without larger voids and the thickness of the external leaves is not less than 75% of the overall thickness of the wall, the entire wall cross section should be considered for the evaluation of the load-bearing capacity (Figure 3).

### 3. Performance properties for multi-leaf masonry

Performance level is an expression of extent of damage to a facility given that a specific earthquake design level affects it. There are differences in expressions for different limit states among researchers as well as in code provisions. While ASCE/SEI 41–06 defines six levels: Immediate occupancy (IO), Damage control range, Life safety (LS), Limited safety range, Collapse prevention (CP), and Not considered—both existing and new EC8-3 use alternative expressions such as Damage limitation (DL), Significant damage (SD), and Near collapse (NC) that may correspond to ASCE/SEI 41–06 limit states IO, LS, and CP. However, limit states stated in ASCE/SEI 41–06 reflect the state of the whole building, considering both structural and non-structural elements, while EC8-3 is oriented solely towards the state of structural elements.

From our test campaign we have identified major crack patterns that may define several limit states (see Table 2 in Kržan and Bosiljkov (2021)). While drift limits at maximum force ( $\theta_{Fmax}$ ) and maximum displacement ( $\theta_{max}$ ) could be associated with SD and NC states, DL could be attributed to either first cracking ( $\theta_{cr}$ ), or elastic displacement ( $\theta_e$ ) (Table 6). Unlike the former state, which may be effectively used when modeling the whole backbone curve of structural element response, elastic displacement

is analytically determined following bi-linear elasto-plastic idealization of the backbone curve and it subsequently does not represent a physical limit state.

Separation of leaves during testing occurred mostly under the higher level of pre-compression and while the specimens were already in softening range (see Table 2 in Kržan and Bosiljkov (2021)); thus, for this type of masonry (inner core < 25% overall thickness), the limit state does not influence the overall capacity of the structural element and the occurrence of specific limit states.

Existing EC8-3 for masonry is rather straightforward and prescribes the same performance limits, regardless of the type of masonry. For the SD limit state, shear and flexural mechanism drifts are limited up to 0.40% and  $h_0/l_w \cdot 0.80\%$  ( $h_0$  being the distance between the section where the flexural capacity is attained and the contra-flexure point), respectively. The NC limit state is defined as the SD state multiplied by 4/3.

ASCE/SEI 41–06 (2007) requirements for the design of new structures are oriented toward contemporary masonry with regular texture and morphology. The shear mechanism is dominant regardless of the type of analysis, while the rocking mechanism could be considered solely for non-linear design. The IO state acceptance criterion for drift is set to 0.1%; for the LS and CP states the criterion is set according to the effective height of elements  $h_{eff}$  (for walls the storey height, for piers the height of openings) as  $h_{eff}/l_w \cdot 0.3\%$  and  $h_{eff}/l_w \cdot 0.4\%$ , respectively. For the rocking mechanism, the softening behavior is limited to  $h_{eff}/l_w \cdot 0.8\%$ . However, when it comes to damage assessment of existing buildings following seismic events, these limits are set to 0.3% for IO, 0.6% for LS, and 1.0% for CP.

Some national codes do not define drift capacity in respect to failure mode, but as the function of applied axial stresses and boundary conditions. SIA code (Pfy-Lang, Braune, and Lestuzzi 2011) defines drift capacity according to Equation 20, where coefficient  $\eta$  is equal to 0.4% and 0.8% for fixed-ends and cantilever boundary conditions, respectively

**Table 5.** In-plane deformation capacities for different limit states of the capacity curve as proposed in the new version of EC8-3.

Masonry	Rocking	Shear sliding	Diagonal cracking
		SD	
Regular	0.01· (1-σ <sub>0</sub> /f <sub>Mc</sub> )	0.40% for hollow units	0.60%
Irregular	0.01· (1-σ <sub>0</sub> /f <sub>Mc</sub> )	0.80% 0.50% for limit value of V <sub>Rd,du</sub> ·f <sub>v</sub>	0.50%
		NC	
Regular	4/3 SD	4/3 SD	4/3 SD
Irregular	4/3 SD	Not applicable	4/3 SD

If shear resistances according to two failure mechanism criteria are within the 10%, the failure may be considered as mixed mode further using a force-deformation relationship in which drift thresholds and strength degradation values result from interpolation between values associated with the two corresponding failure mechanisms.

**Table 6.** Average drifts at characteristic limit states for conducted tests with the same prevailing failure mechanism.

Limit state	First shear crack	Maximum force	Maximum displacement	Elastic displacement
Prevailing failure mechanism	θ <sub>cr</sub> [%] (CV [%])	θ <sub>Fmax</sub> [%] (CV [%])	θ <sub>max</sub> [%] (CV [%])	θ <sub>e</sub> [%] (CV [%])
Rocking	1.74 (33)	3.94 (13)	3.99 (13)	0.73 (34)
Mixed	0.55 (14)	1.71 (12)	1.88 (8)	0.88 (16)
Shear	0.22 (29)	1.10 (23)	1.53 (20)	0.38 (17)

The failure mechanism of walls that was governed by both flexural and shear behaviour is referred to as mixed mechanism. The term mixed failure mode is also introduced in the new EC8-3 proposal for elements in which the shear resistances—according to two failure criteria—are close.

$$\theta_{NC} = \frac{4}{3} \eta (1 - \sigma_0 / f_{Mc}) \quad (20)$$

This last approach was adopted (in a slightly modified form) for the purpose of setting the SD performance limit for the rocking mechanism in the new proposal of EC8-3, where deformation capacities for piers are dependent on the type of failure mechanisms and masonry, and are summarized in Table 5.

Unlike the existing EC8-3, which considers the reduction factor (confidence factor CF) in dependence of the knowledge levels solely for the purpose of assessing the shear resistance, the new proposal has extended this approach to whole capacity, thus also including the reduction of deformation drifts. The new proposal for the determination of masonry elements' deformation capacities in EC8-3 is probabilistically oriented and tries to close the gap in the incomplete knowledge of geometry, constructive details and material properties, by providing a loop between preliminary numerical assessment and in-situ investigations. Thus, for the evaluation of performance limits, different knowledge levels are to be considered as reduction factors. The drift ratio at performance limit “*i*” (*i* = SD, NC) is proposed as

$$\theta = \theta_i / \gamma_{Rd} \quad (21)$$

where  $\gamma_{Rd}$  should be chosen based on the minimum knowledge level of the three: KLG (geometry), KLD (details), and KLM (materials). KLM is to be ignored in the case of NC performance level, since there is no sufficient experimental data for the quantification of the influence of material properties on the ultimate drift ratio. Values for KLG and KLD may vary in the range of 1.70–1.85, depending on the 3 levels of knowledge (C-comprehensive, E-extended, and L-limited), while KLM may vary in the range of 1.5–2.0 for all performance limits except NC.

### 3.1. Lateral drift performance limits of tested piers

The average drifts of piers in both loading directions and various limit states are presented in Table 6 for the tests that exhibited a similar failure mechanism. Ultimate drift values  $\theta_{max}$  obtained for the rocking mechanism significantly exceed the values provided in the codes; they were 2.5 times higher than the recommended values in EC8-3 (EN 2005-3: 2005 2005) and 6.6 times higher than the recommendation for design, as well as 4.0 times higher for damage assessment purposes as stated in ASCE/SEI 41-06 (2007). Drifts  $\theta_e$ , which correspond to elastic displacements of the idealized bi-linear curves and can be compared to the IO drift limit provided in ASCE/SEI 41-06 — equal to 0.1% for design and 0.3% for damage assessment purposes — are on average 7.3 and 2.4 times higher, respectively. In case of shear and flexural mechanisms, SD drift limits provided in current EC8-3 are 2.9 and 4.8 times higher, respectively. In general, it may be concluded that the current code provisions provide very conservative requirements.

## 4. Discussion

### 4.1. Resistance — model error

The obtained masonry compressive strength in the tests coincides with the NTC 2018 (2018) minimum values for dressed rectangular stone. The reason for it being on lower bound could be due to the significant thickness of mortar joints (with regard to dressed masonry). All analytical models for multi-leaf masonry, apart from Binda's model (Binda et al. 2006), significantly underestimate the compressive strength when the external leaf compressive strength  $\gamma_{Rd}$  is set very high. The tests therefore confirm that, for the tested type of masonry and morphology characteristics, i.e., good-quality, ashlar three-leaf stone masonry with a core lacking many voids

(<10%) and thickness of the core less than 25% of the walls' thickness, the masonry can be considered as single-leaf and a reduction of the cross section for the purpose of evaluation of mechanical properties should be avoided.

Comparison of the experimentally obtained lateral resistances showed that a very good correlation to design shear resistances is obtained if the flexural and diagonal cracking (with tensile strength  $f_{Mt}$ ) failure criteria are taken into account. These two failure criteria also accurately predict the failure mechanism, despite being very close to each other for the cantilever boundary conditions and higher vertical load. Predicted shear resistance was conservative in all cases, considering NTC minimum values for  $f_{Mt}$  (also foreseen in the new EC8-3).

According to the new EC8-3 proposal, the shear resistance should be determined as a lower bound considering different failure criteria applied and depending on the type of masonry (regular or irregular texture). Besides the flexural mechanism, diagonal failure (considering  $f_{Mt}$ ) is foreseen for irregular masonry; shear sliding, diagonal failure through joints, and flexural mechanism are foreseen for regular masonry. This analysis confirms that if diagonal failure is omitted, a criterion for diagonal failure through joints is needed, since shear sliding and flexural criteria significantly overestimate the resistance in case of high vertical load and fixed boundary conditions—by 80% in our case. On the other hand, for this case, the diagonal failure through joints provides conservative results and underestimates the resistance for more than 50%. This failure criteria will be always the most critical for masonry made from weak lime mortar and a structural element of this geometry aspect ratio (piers), as it has already been discussed elsewhere (Bosiljkov et al. 2003; Kržan, Žarnić, and Bosiljkov 2011). Shear sliding failure criteria was more critical in comparison to rocking or diagonal only in the case of a very low vertical load (5%  $f_{Mc}$ ).

In the current version of EC8-3, a reduction of the obtained shear resistance of the walls is to be made with regard to the knowledge level of materials, geometry, and details accounting for the uncertainties in the resistance. For this purpose, mechanical parameters are reduced by a Confidence Factor (CF), strictly related to a specific Knowledge Level (KL) and may range from 1.0 for the highest level of KL3 to 1.35 for the lowest KL1. Contrary to current EC8-3, where there is no reduction of resistance for the highest KL, the new EC8-3 proposes the reduction coefficients (partial factor  $\gamma_{Rd}$ , see Equation 19) as 1.35, 1.40, and 1.65, depending on whether sliding, diagonal through joints or flexural criteria are used, respectively—even if the highest KL is considered.

Here, it should be noted that the reduction coefficient  $\gamma_{Rd}$  for structural elements cannot be compared straightforward to CF, since the former is related both to the variability of the parameter and to the sensitivity of the response to the parameter itself (Cattari et al. 2015).

#### 4.2. Performance in terms of deformation capacity

The results of presented tests conducted on historic masonry walls (where ductile mortar governs the overall behaviour) indicate that displacement capacity of well-connected good-quality multi-leaf historic masonry could be significantly underestimated. Similar conclusions were drawn also for modern masonry walls with ductile mortar (Laghi et al. 2020). Since the tested masonry had regular courses and the leaves were well connected with compact infill, the attained high deformation capacity, in comparison to modern masonry, can be attributed to the mortar characteristics. Lime-based mortar in historical structures is weaker but more ductile/less brittle than cement mortar commonly used in modern masonry; it enables a better load transfer in the wall and subsequent failure through the joints. As seen in Figure 4, the damage mechanisms obtained in

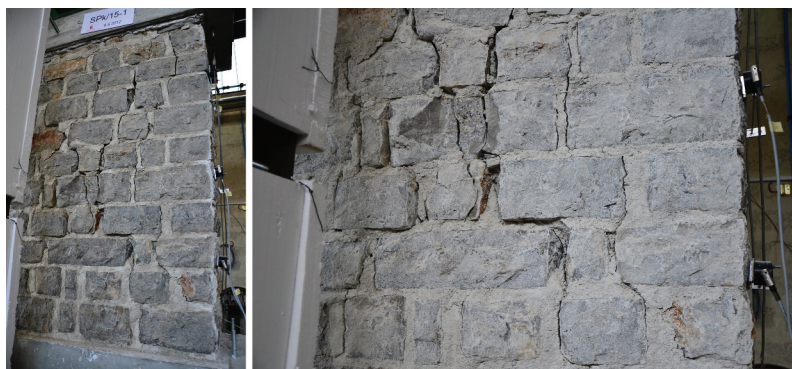


**Figure 4.** Damage mechanism—diagonal failure through joints as well as units enabled by the “ductile” mortar (wall tested under cantilever boundary conditions and 15%  $f_{Mc}$  vertical load).

conducted tests confirm that the soft mortar can enable stress redistribution and propagation of cracks through the units, thus enabling large deformations. This advantage was also recognized in the former Yugoslav codes from 1981 (UL SFRJ 31/81 1981), where it was explicitly stated that pure cement mortar is forbidden in earthquake-prone areas. It should be emphasized, however, that this advantage is valid solely for joints of normal thickness (i.e., up to average thickness 15 mm). For thicker joints (test no. 6 with average joint thickness of 25 mm), substantially lower resistance and displacement capacities were obtained (47% and 41% lower, respectively (Kržan and Bosiljkov 2021)) in comparison to other tests with the same boundary conditions.

From Table 5 it may be concluded that the ultimate drift capacity limits are increased in the new EC-3 proposal. In fact, in design they will be lower, since they are to be reduced according to KL (Equation 21) where the foreseen partial factors  $\gamma_{Rd}$  are 1.7 and 1.85 for the highest and lowest KL, respectively. Furthermore, an additional  $\gamma_{Rd}$  is foreseen for the reduction of the global deformation capacity of the whole structure in dependence of KL; it is in the range of 1.70–1.90. One of the possibilities for solving this issue would be to provide drift limits in dependence of the type and quality of the masonry. Another option could be to determine possible higher upper-bound limits with a smaller reduction of deformation capacity in the cases where higher drift capacity is proven by in-situ or laboratory experimental tests.

An additional action that may slightly compensate the increased demand for global capacity of the structure is to choose a higher reduction (behaviour factor  $q$ ) of design response spectra. In the existing EC8-1 (EN 2004-1:2004 2004), the  $q$  for an URM (unreinforced masonry) building is a national parameter set as a single value in the range of 1.5–2.5, with a recommended lower bound value. In the new version of EC8-1-2 (prEN 1998-1-2:2019.3 2019), this will be determined directly according to code provisions (considering deformation capacity, energy dissipation, and overstrength)—again in the range of 1.5–2.5 with a possibility to choose an upper bound value. Furthermore, the seismic demand could be reduced by introducing factor  $\delta$ , a coefficient that depends on the consequence class of the considered structure and would be determined as a national parameter. Although it is unlikely that it will be used for ordinary existing buildings, this coefficient may help in reducing demand for cultural heritage and monument buildings.

### 4.3. Stiffness characteristics

Another important issue recognised from the test result analysis is the prediction of the walls' effective stiffness. The effective stiffness is a complex parameter associated with all restoring forces of structural system and depends upon several factors including different failure mechanisms (Bosiljkov, Totoev, and Nichols 2005). The tests have undoubtedly shown that in reality, due to soft mortar, fixed-fixed boundary conditions can be unrealistic for historical masonry, since the soft mortar has plastic behavior from the early stage of loading and enables rotation of the stone units at the joint level due to extensive crushing and loss of mortar from the joints. It was shown for the tested walls (more details in Kržan and Bosiljkov (2021)) that better correspondence of predicted and experimental effective stiffnesses is obtained by neglecting the fixed boundary conditions (i.e., analytically predicted effective stiffnesses 21.5 kN/mm and 49.0 kN/mm in comparison to average experimental values 20.4 kN/mm and 21.2 kN/mm for walls with high precompression and cantilever and fixed-fixed boundary conditions, respectively). The same may be applied concerning the evaluation of masonry shear modulus from experimental cyclic shear tests; more consistent results are obtained if fixed boundary conditions are neglected.

### 4.4. Reliability of test data

It is well known that, due to the nonhomogeneous nature of masonry, expected characteristics cannot be determined with a high level of precision and certainty. This is also apparent from the results of performed tests, where all masonry specimens were constructed by the same group of stone masons using the same materials. All of the specimens were cured and tested in laboratory conditions.

In spite of that, a relatively large scatter of the results was obtained (up to 12% CV for the  $F_{max}$  resistance and up to 20% for deformation capacity). These results are better than some of our other results where a higher CV was noted on URM masonry made from solid brick units (18% for  $F_{max}$  and 30% for deformation capacity (Bosiljkov et al. 2003)) and blockwork masonry (15% for  $F_{max}$  and 34% for deformation capacity (Kržan, Žarnić, and Bosiljkov 2011)). In general, it may be concluded that a higher scattering of results may be expected for deformation parameters.

Another major obstacle—prior to implementation of the effective probability approach in seismic design—is

defining harmonized test methods for the evaluation of important parameters for PBA. There are numerous different test set-ups, but none of them can simulate real conditions. Still, they have all been chosen because they reproduce static or kinematics boundary conditions which can be easily interpreted and reproduced. The results of all tests are therefore not directly comparable (Borri, Castori, and Corradi 2015). Furthermore, the idealization and interpretation of performance limits are done in accordance with the current state-of-the-art or common practice, which may again significantly influence the comparison and interpretation of obtained results (Vanin et al. 2017).

## 5. Conclusions

The paper critically evaluates the performance of multi-leaf stone masonry with an inner core of less than 25% of the wall's overall thickness that was in detail presented in Kržan and Bosiljkov (2021), with regard to the performance limits and methodology for their evaluation stated in the current (EC8-3) and the forthcoming second generation of Eurocodes (new proposal of EC8-3) as well as in ASCE/SEI 41-06 (former FEMA 536) code provisions.

The new proposal of EC8-3 is probabilistically oriented and considers different (both aleatoric and epistemic) uncertainties in defining input parameters. To consider the high level of uncertainties, partial factors are defined in the proposal, depending on KL for materials, details, and geometry; they may also vary according to the type of analysis. The factors are applied to define the capacity of structural elements for both mean characteristics and mean deformation values. Mean values for mechanical characteristics are provided in the proposal together with their standard deviation in case there is no sufficient experimental data available. This whole new approach is designed so that the characteristics of the structure's strong entities could be lowered towards the mean, while the characteristics of weak entities (critical ones) could be raised towards the same mean. On average, new analyses should enable a stronger structure.

Consequently, new partial factors are higher than 1.0 for even the highest knowledge levels. Our test results indicate, however, that they might be very conservative. The test results provide a much higher deformation capacity than the limits provided in both the new proposal of EC8-3 as well as those in the current EC8-3 and ASCE code provisions. The reason for the high deformation capacity of the tested masonry lies in the soft, "ductile" mortar for which, the presumed deformation capacity could/should be higher for good

quality masonry—as stated in the code provisions. Another important conclusion regarding the soft mortar is that it influences the boundary conditions. While the proposed approach in new EC8-3 would lead to a safer structure, one should be aware that the high partial factors would make it even harder (if at all possible) to achieve the seismic demands for the buildings that are here around us already for hundred years. This approach may lead to rigorous strengthening measures which are not desirable or feasible for many historical structures, resulting in unacceptable costs of retrofitting.

The analysis of proposed shear resistance models in the new EC8-3 showed that a good correspondence with test results is obtained with diagonal cracking (of homogenised masonry) criterion and flexural criterion. On the other hand, diagonal failure through joints provides very conservative results and underestimates the resistance for more than 50%. These failure criteria will always be the most critical for masonry made from weak lime mortar and a structural element of this geometry aspect ratio (piers).

Classification of existing (old) masonry in the new proposal of EC8-3 is mostly based on Italian code provisions NTC 2018. All provided data is applicable to normal bed joint thicknesses with some correction factors for thin bed joints (<10 mm). From our tests, it was shown that the thicker joints (>25 mm) may significantly influence the seismic capacity of masonry piers. This and other influencing parameters may be studied solely through laboratory or in-situ testing. Most of the time it is hard to reproduce existing historical masonry in laboratory conditions, thus in-situ destructive testing is inevitable. Results obtained from in-situ tests would decrease uncertainties regarding input parameters, but they would be ultimately severely reduced by the high partial factor as proposed in new EC8-3.

The values proposed for reduction coefficients, for both mechanical parameters and drift limits that depend on knowledge levels, are set very high and will discourage any further in-situ destructive testing on existing historical masonry. These tests are costly and, in the long term, this will present a major obstacle in enriching the world database of experimental results for different types of masonry.

## Acknowledgments

The tests were conducted within the project PERPETUATE, funded by the European Commission in the 7th Framework Programme under grant agreement n° 244229. The financial

support of Slovenian Research Agency through P2-0185 (B) is gratefully acknowledged.

## Disclosure statement

No potential conflict of interest was reported by the author(s).

## References

- Aničić, D., Z. Sorić, D. Morić, and H. Macan. 1989. Mechanical properties of stone masonry walls. In *Structural repair and maintenance of historical buildings*, ed. C. A. Brebbia, 95–102. Basel: Computational Mechanics Publications; Birkhäuser.
- ASCE/SEI 41–06. 2007. *Seismic rehabilitation of existing buildings (ASCE/SEI 41–06)*. Reston, VA: Seismic Rehabilitation Standards Committee, American Society of Civil Engineers.
- Binda, L., A. Fontana, and L. Anti. 1992. Load transfer in multiple leaf masonry walls. Paper presented at the International Workshop Effectiveness of injection techniques for retrofitting of stone and brick masonry walls in seismic areas, Milan, Italy.
- Binda, L., J. Pina-Henriques, A. Anzani, A. Fontana, and P. B. Lourenço. 2006. A contribution for the understanding of load-transfer mechanisms in multi-leaf masonry walls: Testing and modelling. *Engineering Structures* 28 (8):1132–48. doi:10.1016/j.engstruct.2005.12.004.
- Borri, A., G. Castori, and M. Corradi. 2015. Determination of shear strength of masonry panels through different tests. *International Journal of Architectural Heritage* 9 (8):913–27. doi:10.1080/15583058.2013.804607.
- Bosiljkov, V., A. Page, V. Bokan-Bosiljkov, and R. Žarnić. 2003. Performance based studies of in-plane loaded unreinforced masonry walls. *Masonry International* 16:39–50.
- Bosiljkov, V., M. Tomaževič, U. Bohinc, and I. Leskovic. 2004. On-site investigation techniques for the structural evaluation of historic masonry buildings. Deliverable D10.2 & 10.4. Report on the evaluation at pilot sites (Report for owners of historic buildings): Pilot site: Pišce/Slovenia: Revised report. ONSITEFORMASONRY project, 178. Ljubljana: Zavod za gradbeništvo Slovenije.
- Bosiljkov, V., Y. Z. Totoev, and J. M. Nichols. 2005. Shear modulus and stiffness of brickwork masonry: An experimental perspective. *Structural Engineering and Mechanics* 20 (1):21–43. doi:10.12989/sem.2005.20.1.021.
- Cattari, S., S. Lagomarsino, V. Bosiljkov, and D. D’Ayala. 2015. Sensitivity analysis for setting up the investigation protocol and defining proper confidence factors for masonry buildings. *Bulletin of Earthquake Engineering* 13 (1):129–51. doi:10.1007/s10518-014-9648-3.
- DIN 1053-1: 1996-11. 1996. *Mauerwerk - Teil 1: Berechnung und Ausführung*. Berlin: Institut für Normung e.V.: Beuth Verlag.
- Egermann, R. 1993. Investigation on the load bearing behaviour of multiple leaf masonry. *IABSE reports = Rapports AIPC = IVBH Berichte* 70. doi:10.5169/seals-53311.
- Elmshawi, A., D. Duchesne, J. Paquette, A. Mufti, L. Jaeger, and N. Shrive. 2011. Elastic moduli of stone masonry based on static and dynamic tests. Paper presented at the 11th NAMC, Minneapolis, USA.
- EN 1996-1-1: 2005. 2005. *Eurocode 6: Design of masonry structures – Part 1-1: General rules for reinforced and unreinforced masonry structures*. Brussels, Belgium: CEN.
- EN 1998-1:2004. 2004. *Eurocode 8: Design of structures for earthquake resistance - Part 1: General rules, seismic actions and rules for buildings*. Brussels, Belgium: CEN.
- EN 1998-3: 2005. 2005. *Eurocode 8: Design of structures for earthquake resistance – Part 3: Assessment and retrofitting of buildings*. Brussels, Belgium: CEN.
- EN1998-3 SC8 06-10-2019. 2019. *Eurocode 8: Design of structures for earthquake resistance – Part 3: Assessment and retrofitting of buildings and bridges*. CEN/TC 250/SC 8: CEN.
- Franchin, P., P. E. Pinto, and P. Rajeev. 2010. Confidence factor? *Journal of Earthquake Engineering* 14 (7):989–1007. doi:10.1080/13632460903527948.
- Kržan, M., R. Žarnić, and V. Bosiljkov. 2011. Design of lateral resistance of URM blockwork through theoretical models and code provisions. Paper presented at the 9th Australasian masonry conference, Queenstown, New Zealand.
- Kržan, M., and V. Bosiljkov. 2021. Compression and in-plane seismic behaviour of ashlar three-leaf stone masonry walls. *Manuscript Submitted for Publication to International Journal of Architectural Heritage*.
- Laghi, V., M. Palermo, A. Incerti, G. Gasparini, and T. Trombetti. 2020. High performance mortar for ductile seismic-resistant unreinforced masonry systems. *Construction and Building Materials* 245:118385. doi:10.1016/j.conbuildmat.2020.118385.
- Magenes, G., A. Galasco, A. Penna, and M. Da Paré. 2010. In-plane cyclic shear tests of undressed double leaf stone masonry panels (paper no. 1435). Paper presented at the 14th European conference on earthquake engineering, Ohrid, FYROM.
- Mann, W., and H. Müller. 1982. Failure of shear-stressed masonry - an enlarged theory, tests and application to shear walls. In *Proceedings of the British ceramic society: Load-bearing brickwork*, ed. H. W. H. West, 223–35. Stoke-on-Trent, England: British Ceramic Society.
- NTC 2008. 2009. Istruzioni per l’applicazione delle nuove norme tecniche per le costruzioni di cui al Decreto Ministeriale 14 Gennaio 2008 Circ. C.S.LL.Pp. No. 617 of 2/2/2009, MIT.
- NTC 2018. 2018. D.M. del Ministero delle Infrastrutture e dei trasporti del 17/01/2018. Aggiornamento delle Norme Tecniche per le Costruzioni (in Italian), MIT.
- Pfyll-Lang, K., F. Braune, and P. Lestuzzi. 2011. SIA D 0237: Evaluation de la sécurité parasismique des bâtiments en maçonnerie. *Documentation SIA D 237*. Zürich, Switzerland.
- PIET 70. 1971. *Obras de fábrica. Prescripciones del Instituto Eduardo Torroja*. Madrid, Spain: Consejo Superior de Investigaciones Científicas.
- prEN 1998-1-2:2019.3. 2019. *Eurocode 8: — Design of structures for earthquake resistance — Part 1-2: Rules for new buildings*. CEN/TC 250/SC 8, CEN.
- Tassios, T. 2004. Recupero di murature tri-strato (Rehabilitation of three-leaf masonry). In *Evoluzione nella sperimentazione per le costruzioni, seminario internazionale*, 26 Sept- 3 Oct., Centro Internazionale di Aggiornamento Sperimentale – Scientifico (CIAS). 137–63. Bolzano, Italy.

- Tassios, T., and M. Chronopoulos. 1986. Aseismic dimensioning of interventions on low-strength masonry buildings. Paper presented at the Middle east and mediterranean regional conference on low strength masonry in seismic areas, Middle East Technical University, Ankara.
- Tomažević, M. 1999. *Earthquake-resistant design of masonry buildings*. London, UK: Imperial College Press.
- Turnšek, V., and F. Čačovič. 1971. Some experimental results on the strength of brick masonry walls. Paper presented at the 2nd International Brick Masonry Conference, Stoke-on-Trent.
- UL SFRJ 31/81. 1981. Pravilnik o tehničnih normativih za graditev objektov visoke gradnje na seizmičnih območjih. UL SFRJ 31/81, Spremembe in dopolnitve: UL SFRJ 49/82, 29/83, 21/88, 52/90.
- Vanin, F., D. Zaganelli, A. Penna, and K. Beyer. 2017. Estimates for the stiffness, strength and drift capacity of stone masonry walls based on 123 quasi-static cyclic tests reported in the literature. *Bulletin of Earthquake Engineering* 15 (12):5435–79. doi:10.1007/s10518-017-0188-5.